

Characterization and carbon monoxide oxidation activity of $\text{La}_{1-y}\text{Sr}_y\text{Cr}_{1-x}\text{Ru}_x\text{O}_3$ perovskites

A. TERLECKI-BARIČEVIĆ, S. PETROVIĆ, D. JOVANOVIĆ, LJ. KARANOVIĆ*
and C. MARINOVA**

ICTM-Department of Catalysis and Chemical Engineering, Njegoševa 12, YU-11000 Belgrade,
**Laboratory of Crystallography, Faculty of Mining and Geology, University of Belgrade, Đušina 7,*
*YU-11000 Belgrade, Yugoslavia and **Institute of General and Inorganic Chemistry, BAN,*
1113 Sofia, Bulgaria

(Received 6 July 1999)

The oxidation of CO over $\text{La}_{1-y}\text{Sr}_y\text{Cr}_{1-x}\text{Ru}_x\text{O}_3$ perovskite type oxides with $y=0.3$ and $0 \leq x \leq 0.100$ have been studied. X-ray fluorescence analysis confirmed that content of elements in the bulk corresponds to the established nominal perovskite stoichiometry, indicating that no significant oxidation of ruthenium into volatile polyvalent oxides with their consequent escape from the sample occurred in air up to the temperature of 1000 °C. According to X-ray diffraction analysis, all samples achieved the perovskite hexagonal with the presence of some SrCrO_4 . X-ray photoelectron spectroscopy analysis of ruthenium samples shows higher Ru and Sr surface concentrations than in the bulk. The binding energy for Ru_{3p} is virtually the same in all samples and consistent with that of Ru^{4+} (463.6–464.3 eV). Kinetic studies were performed in a differential recycle reactor with a recycling ratio 80. The results show that substitution of Ru^{4+} for Cr^{3+} in $\text{La}_{1-y}\text{Sr}_y\text{CrO}_3$ leads to a significant increase in both the activity and the activation energy. The global CO oxidation rate, referred on the BET surface area, correlates with the surface Ru^{4+} atomic concentration. Hence, the activity reflects the surface enrichment in ruthenium. Moreover, an identical apparent activation energy $E = 93$ kJ/mol and the same specific rate per ruthenium surface ion were obtained for samples with a Ru content $x \pm 0.05$ suggest that exposed Ru^{4+} ions mainly participate in the reaction.

Keywords: perovskite, ruthenium, CO oxidation.

Studies of perovskite type catalysts (ABO_3) with a rare earth ion in the A site and a transition metal ion in the B site have concentrated on the complete oxidation of CO and hydrocarbons and reduction of NO_x particularly related to auto exhaust control.^{1,2}

In our previous papers^{3–5} we reported on the activity of a series of LaMO_3 ($M = \text{Co}, \text{Cr}$ and Cu) perovskites and mixed oxides $\text{La}_{1-y}\text{Sr}_y\text{MO}_3$ ($M = \text{Cr}$ and Ru) in the simultaneous oxidation of CO and hydrocarbons and reduction of NO_x with controlled compositions of the gas mixture around the stoichiometric ratio of

oxidizing to reducing agents. The investigations were performed in a pulse-flame catalytic system⁶ with a feed gas obtained by combustion of 2,2,4 trimethylpentane (isooctane) containing about 11 vol.% of H₂O and also in a dry synthetic gas mixture. According to the results on La_{1-y}Sr_yCr_{1-x}Ru_xO₃ (0.05 ≤ x ≤ 0.100) mixed oxides, under net reducing conditions, an unexpected higher conversion of CO and a higher concentration of hydrogen in the outlet reaction gases were obtained in the presence of water vapor compared to those observed in the synthetic dry reaction mixture. These effects were ascribed to the water-gas shift reaction, catalyzed by ruthenium ions. Furthermore, the hydrogen formed in the water gas shift reaction, absorbed on the surface in the dissociative form, could be a reason for the high conversion of NO_x observed on ruthenium perovskites under net oxidizing conditions.

This paper presents the CO oxidation activity of perovskite type oxides La_{1-y}Sr_yCr_{1-x}Ru_xO₃ with y = 0.3 and 0 ≤ x ≤ 0.100. The results are discussed in relation to the bulk and surface composition and the oxidation state of the cations in samples with different Ru content.

EXPERIMENTAL

Catalyst preparation

A series of perovskite type oxides La_{1-y}Sr_yCr_{1-x}Ru_xO₃ containing a constant content of Sr (y = 0.3) and with x ranging from 0 to 0.100 was prepared from La₂O₃, Cr₂O₃, RuO₂ and SrCO₃ of analytical grade quality by solid state processing. The respective amounts of the constituent oxides and carbonates were mixed in ethanol and sintered. The temperature of calcination was increased stepwise up to 1000 °C. Cycles of grinding and heating were performed at the chosen temperatures to ensure homogeneity and to complete the reaction.⁷

Characterization of catalyst

The chemical composition of the samples was determined by X-ray fluorescence analysis (XRF), using a System Cambera Model 7333 E. The phase composition of the samples was investigated by X-ray diffraction analysis (XRD) of powdered samples using a Philips PW 1710 diffractometer, with CuKα graphite-monochromatized radiation (40 kV, 30 mA). The lattice constants were calculated by the least squares method (program LSUCRIPC).⁸ X-ray photoelectron spectra (XPS) were recorded on a VC Escalab II spectrometer with MgKα radiation (1253.6 eV) at a pressure of 4 · 10⁻¹¹ Torr and an instrumental resolution for Ag 3d_{3/2} line 0.9 eV. The normalized XPS intensities I/s, which are proportional to the effective concentrations of the corresponding elements in the surface layers,⁹ were determined as the integrated peak areas divided by the corresponding photon ionization cross section σ.¹⁰ In the peak area computation, the background was assumed to be linear.

The specific surface area of the samples was measured using the BET method.

Catalytic tests

The kinetics of carbon monoxide oxidation was measured in an integrated-external recycle reactor. A detailed description of the apparatus has been given elsewhere.^{11,12} A reaction gas mixture containing 1 vol.% CO and 1 vol.% O₂ was fed at constant flow rate of 10 l/h. The recycling ratio of 80 was maintained constant to obtain gradientless conditions in all catalytic runs. The gas composition was analyzed before and after the reaction by an online gas chromatograph (Shimadzu GC-8A) interfaced with an automatic integrator. The global reaction rate was calculated using the equation:

$$r = ((c_{\text{CO}}^0 - c_{\text{CO}})/w) \cdot F$$

where c_{co}^0 and c_{co} are the concentration of CO (vol.%) in the inlet and the outlet, respectively, w is the mass (g) of catalyst, and F is the feed flow rate (cm^3/s).

RESULTS AND DISCUSSION

The atomic concentrations of elements in the bulk (XRF) and the surface layers (XPS) of the ruthenium perovskites are given in Table I.

TABLE I. Bulk and surface concentrations of the elements in $\text{La}_{1-y}\text{Sr}_y\text{Cr}_{1-x}\text{Ru}_x\text{O}_3$ ($y = 0.3$; $0.025 \leq x \leq 0.100$) samples

x	Bulk concentration (at.%)					Surface concentration (at. %)				
	La	Sr	Cr	Ru	O	La	Sr	Cr	Ru	O
0.025	14.0	6.0	19.5	0.5	60.0	10.0	7.2	9.8	0.8	72.2
0.050	14.0	6.0	19.0	1.0	60.0	11.0	7.8	10.0	2.0	69.2
0.075	14.0	6.0	18.5	1.5	60.0	9.4	8.9	9.2	3.6	68.9
0.100	14.0	6.0	18.0	2.0	60.0	8.1	11.1	9.5	3.8	67.5

The content of elements in the bulk corresponds to the composition of the initial mixture of the samples, *i.e.*, to the nominal perovskite stoichiometry $\text{La}_{1-y}\text{Sr}_y\text{Cr}_{1-x}\text{Ru}_x\text{O}_3$ with $y = 0.3$ and x varying in the range $0.025 \leq x \leq 0.100$. Moreover, the very good agreement between the amounts of ruthenium taken and those found in the systems obtained after heating at 1000°C in air, indicates that no significant oxidation of ruthenium into volatile polyvalent oxides RuO_3 and RuO_4 and their consequential escape from the sample occurred under the oxidation conditions. This is the main problem in the case of supported ruthenium catalysts. In the following figures and tables all the synthesized ruthenium perovskite catalysts are denoted according to the nominal perovskite stoichiometry.

On the XRD pattern (Fig. 1) of the sample without Sr, only perovskite phase LaCrO_3 was identified. The unambiguous phase identification of a few very weak peaks was not possible. The X-ray diffraction peaks of LaCrO_3 were completely indexed from a cubic symmetry with lattice parameter $a = 3.8847(6)\text{\AA}$. In all samples with La partly substituted by Sr in A site, however, weak diffraction peaks attributed to SrCrO_4 were detected together with the perovskite ones. Thermal treatment of the samples in air resulted in the oxidation of part of the Cr^{3+} to Cr^{6+} which reacted with strontium carbonate forming a SrCrO_4 phase.¹³ In the ruthenium containing samples no peaks corresponding to RuO_2 or other component single oxides were detected. Since, according to chemical analysis, almost all ruthenium remained in the samples, the formation of very small RuO_2 particles, which could not be detected by XRD, due to their strong tendency to volatilization under oxidizing conditions, can be excluded. Hence, it can be considered that the ruthenium is incorporated in the perovskite structure.

The formation of SrCrO_4 as a separate phase implies a decrease in the Sr and Cr content in the perovskite phase.

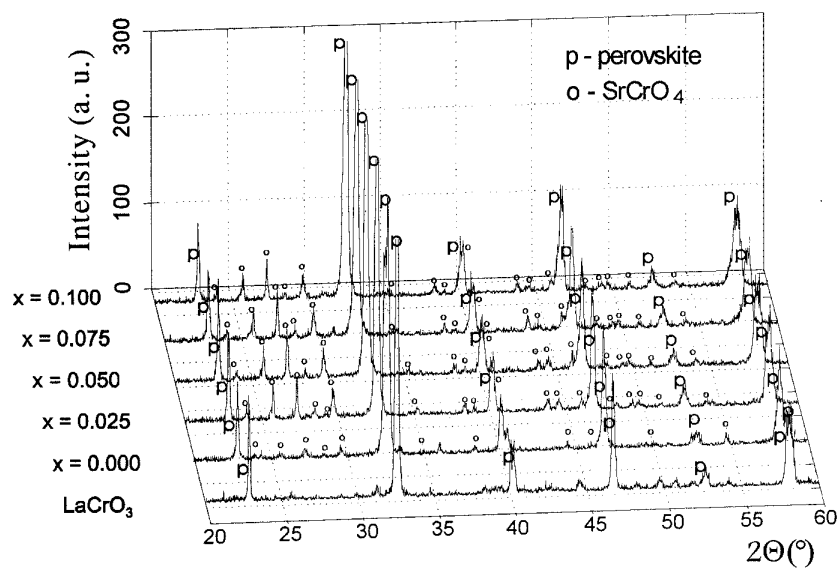


Fig. 1. XRD powder patterns of $\text{La}_{0.7}\text{Sr}_{0.3}\text{Cr}_{1-x}\text{Ru}_x\text{O}_3$ ($0.025 \leq x \leq 0.100$).

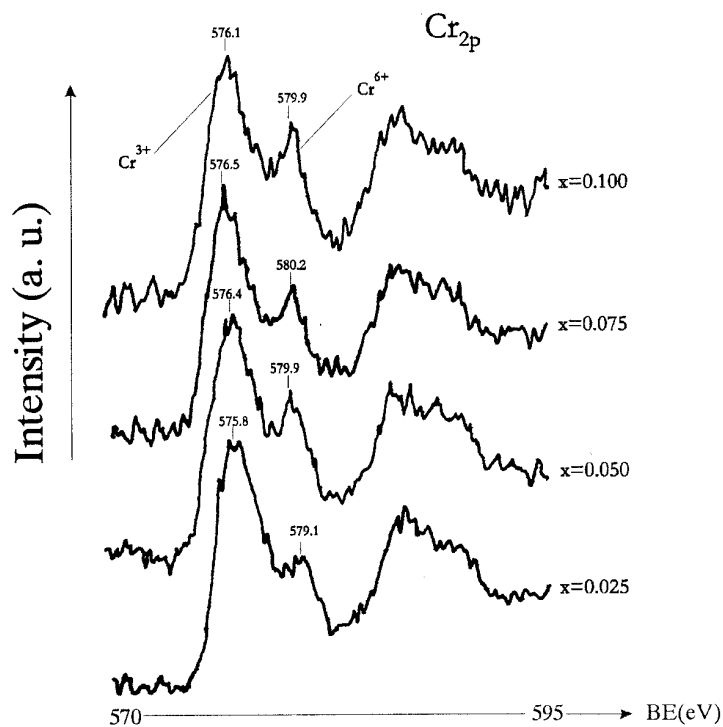


Fig. 2. Photoelectron spectra of Cr_{2p} of $\text{La}_{1-y}\text{Sr}_y\text{Cr}_{1-x}\text{Ru}_x\text{O}_3$ ($0.025 \leq x \leq 0.100$).

The Cr_{2p} photoelectron spectra (Fig. 2) exhibit two peaks with BE of 576.5 eV and 579.9 eV, characteristic for Cr^{3+} and Cr^{6+} , respectively. Standardization of the peaks gave about 20% contribution of Cr^{6+} to the total amount of chromium in the surface layers in all synthesized samples. This is in good agreement with the estimation of the relative bulk content of the SrCrO_4 phase.

The absence of other isolated phases of the individual oxides, which should crystallize out at the calcination temperature of 1000 °C, implies that chromium and equivalent amounts of strontium are distributed in the perovskite and strontium chromate phases. Assuming that 20% of the total amount of Cr (all the formed Cr^{6+}) and an equivalent amount of Sr^{2+} are bonded in SrCrO_4 the calculated average content of Sr in the $\text{La}_{1-y}\text{Sr}_y\text{Cr}_{1-x}\text{Ru}_x\text{O}_3$ perovskite phase significantly decreases from $y=0.3$ to $y=0.14$. Accordingly the La/Sr ratio in the perovskite phase increases from a nominal 2.33 to 6.14.

This is consistent with the lattice parameters of the perovskites $\text{La}_{1-y}\text{Sr}_y\text{Ru}_x\text{Cr}_{1-x}\text{O}_3$, which are given in Table II.

TABLE II. The unit cell parameters of the perovskite phase occurring in the synthesized $\text{La}_{1-y}\text{Sr}_y\text{Cr}_{1-x}\text{Ru}_x\text{O}_3$ samples

The composition of the initial mixtures		Lattice parameters		Volume (\AA^3)	Reference
y	x	$a(\text{\AA})$	$c(\text{\AA})$		
0	0	5.494 [#]	13.458 [#]	352 [6 · 58.62(3)]	this paper
0.3	0.100	5.482(3)	13.504(9)	351.4(4)	this paper
0.3	0.075	5.478(4)	13.495(9)	350.7(4)	this paper
0.3	0.050	5.474(4)	13.48(1)	349.7(5)	this paper
0.3	0.025	5.475(3)	13.488(7)	350.2(3)	this paper
0.3	0	5.466(3)	13.49(1)	349.2(4)	this paper
0.25	0	5.493–0.002 [*]	13.301–0.006	348	JCPDS 32-1240

[#]Calculated from cubic cell with $a = 3.8847(6) \text{ \AA}$ using equations $a = a_c \cdot (2)^{1/2}$ and $c = a_c \cdot (3)^{1/2}/2$.

^{*}Actually, 5.403–0.002 \AA was reported (Khattak,¹⁴) but this is probably a typing error, because the calculated parameter of the hexagonal unit cell from the rhombohedral lattice parameters is $a = 2 \cdot 5.451 \cdot \sin(30.255) = 5.493 \text{ \AA}$.

The observed diffraction peaks of the perovskite phase are mostly broad and asymmetric but not split very well suggesting that the perovskite lattice is slightly distorted compared to an ideal cubic structure. The lattice parameters of the hexagonal perovskite unit cell are very similar for all investigated samples. Moreover, their unit cell volumes are between the LaCrO_3 and the $\text{La}_{0.75}\text{Sr}_{0.25}\text{CrO}_3$ volume.¹⁴ This is in agreement with the previous conclusion concerning the formation of the perovskite phase with a lower content of Sr ($y = 0.14$) than expected ($y = 0.3$) according to the overall metal content (Table I).

The Cr_{2p} binding energy values for Cr^{3+} and Cr^{4+} are very close. Therefore, the separation of the peaks was not possible with the resolution of instrument used. Decon-

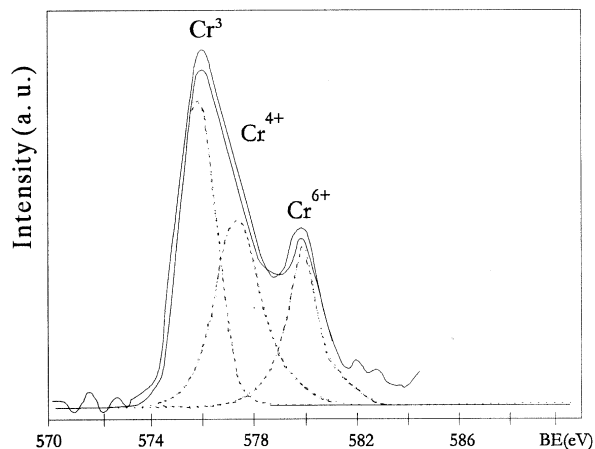


Fig. 3. Photoelectron spectra of Cr_{2p} of Cr^{3+} and Cr^{6+} ions.

olution of the Cr^{3+} peak, which is broad and asymmetric (Fig. 2), performed for the sample $x = 0.075$, might be an indication of the possible presence of Cr^{4+} ions (Fig. 3).

The binding energy for Ru_{3p} (463.6–464.3 eV) is virtually the same in all samples and it is consistent with that of Ru^{4+} (Fig. 4).

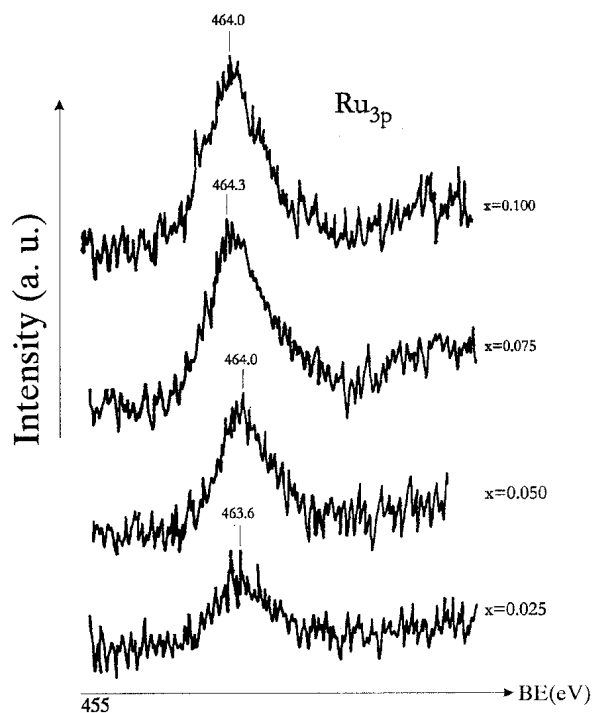


Fig. 4. Photoelectron spectra of Ru_{3p} of $\text{La}_{1-y}\text{Sr}_y\text{Cr}_{1-x}\text{Ru}_x\text{O}_3$ (with $0.025 \leq x \leq 0.100$).

The calculated composition of the perovskite phases in the $\text{La}_{1-y}\text{Sr}_y\text{Cr}_{1-x}\text{Ru}_x\text{O}_3$ samples was made assuming that all Ru is incorporated in the perovskite and is presented in Table III.

TABLE III. Calculated composition of perovskite $\text{La}_{1-y}\text{Sr}_y\text{Cr}_{1-x}\text{Ru}_x\text{O}_3$ phases

x	Calculated composition of the perovskite phases	δ
0	$\text{La}^{3+}_{0.875}\text{Sr}^{2+}_{0.125}\text{Cr}^{3+}_{0.875}\text{O}_{3-\delta}$ $\text{La}^{3+}_{0.875}\text{Sr}^{2+}_{0.125}\text{Cr}^{3+}_{0.875}\text{Cr}^{4+}_{0.125}\text{O}_3$	0.063
0.025	$\text{La}^{3+}_{0.869}\text{Sr}^{2+}_{0.131}\text{Cr}^{3+}_{0.869}\text{Ru}^{4+}_{0.031}\text{O}_{3-\delta}$ $\text{La}^{3+}_{0.869}\text{Sr}^{2+}_{0.131}\text{Cr}^{3+}_{0.869}\text{Cr}^{4+}_{0.100}\text{Ru}^{4+}_{0.031}\text{O}_3$	0.051
0.050	$\text{La}^{3+}_{0.865}\text{Sr}^{2+}_{0.135}\text{Cr}^{3+}_{0.865}\text{Ru}^{4+}_{0.062}\text{O}_{3-\delta}$ $\text{La}^{3+}_{0.865}\text{Sr}^{2+}_{0.135}\text{Cr}^{3+}_{0.865}\text{Cr}^{4+}_{0.073}\text{Ru}^{4+}_{0.062}\text{O}_3$	0.037
0.075	$\text{La}^{3+}_{0.859}\text{Sr}^{2+}_{0.141}\text{Cr}^{3+}_{0.859}\text{Ru}^{4+}_{0.092}\text{O}_{3-\delta}$ $\text{La}^{3+}_{0.859}\text{Sr}^{2+}_{0.141}\text{Cr}^{3+}_{0.859}\text{Cr}^{4+}_{0.049}\text{Ru}^{4+}_{0.092}\text{O}_3$	0.025
0.100	$\text{La}^{3+}_{0.854}\text{Sr}^{2+}_{0.146}\text{Cr}^{3+}_{0.854}\text{Ru}^{4+}_{0.122}\text{O}_{3-\delta}$ $\text{La}^{3+}_{0.854}\text{Sr}^{2+}_{0.146}\text{Cr}^{3+}_{0.854}\text{Cr}^{4+}_{0.024}\text{Ru}^{4+}_{0.122}\text{O}_3$	0.012

The substitution of divalent Sr for trivalent La requires charge compensation, which can be achieved by the formation of either tetravalent chromium or oxygen vacancies.

The partial substitution of divalent Sr for trivalent La in LaCrO_3 leads to the some decrease in unit cell volume despite the fact that Sr^{2+} is a larger ion and has a lower valence state. A probably explanation of this lies in the formation of Cr^{4+} (having a lower ionic radius than Cr^{3+}) which compensates for either steric and electronic effects of Sr^{2+} doping. The formation of certain amount of oxygen vacancies, however, can not be excluded.

However, the progressive substitution of Cr^{3+} for Ru^{4+} (having almost the same ionic radius) in the B position of $\text{La}_{1-y}\text{Sr}_y\text{CrO}_3$ phase simply decreases the need for Cr^{4+} and causes an increase in the unit cell volume (Table II). As a result of the above effect, a decrease in the Ru content reduces the unit cell volume to the smallest value for $x = 0$. The further decrease of the unit cell volume observed in the sample with higher Sr content ($y = 0.25$) can be ascribed to the increase of Cr^{4+} in the some proportion of the Sr^{2+} content.

The O_{1s} photoelectron spectra of the ruthenium catalysts (Fig. 5) indicate that at least two kinds of oxygen species are present on the surface. The lower binding energy of O_{1s} (529.0–529.5 eV) is attributed to lattice oxygen. A shoulder around $\text{BE} = 530.5$ eV, clearly pronounced only for the sample with $x = 0.025$ could be assigned to the absorbed oxygen according to Seiyama.¹⁵

Oxygen sorptive properties of $\text{La}_{1-y}\text{Sr}_y\text{Cr}_{1-x}\text{Ru}_x\text{O}_3$ ($0 \leq x \leq 0.100$) samples in relation to structural defects and the role of absorbed oxygen in the activity and kinetics of CO oxidation is the subject a separate study.

The stabilization of ruthenium ions by incorporating them in the perovskite structure enables the oxidation activity to be investigated with no significant loss of Ru.

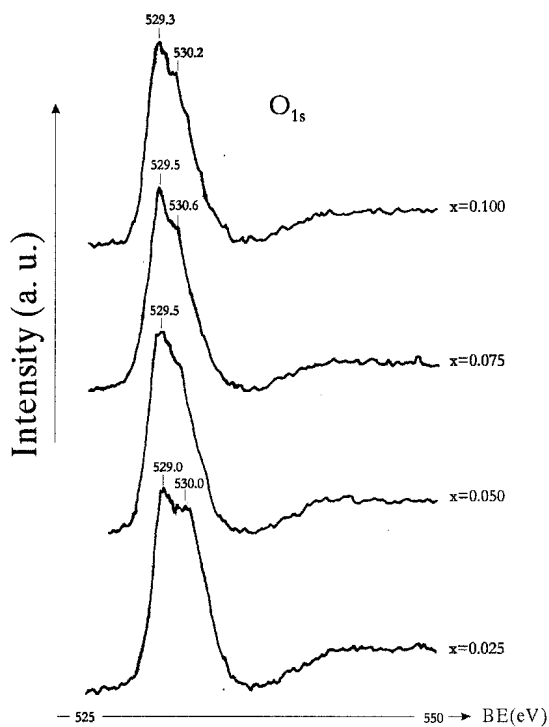


Fig. 5. Photoelectron spectra of O_{1s} of $La_{1-y}Sr_yCr_{1-x}Ru_xO_3$ ($0.025 \leq x \leq 0.100$).

The effect of temperature on the rate of CO oxidation was studied on $La_{1-y}Sr_yCrO_3$ and a series of ruthenium samples in the temperature range of 100 °C to 300 °C using a $CO/O_2 = 1$ reaction gas mixture.

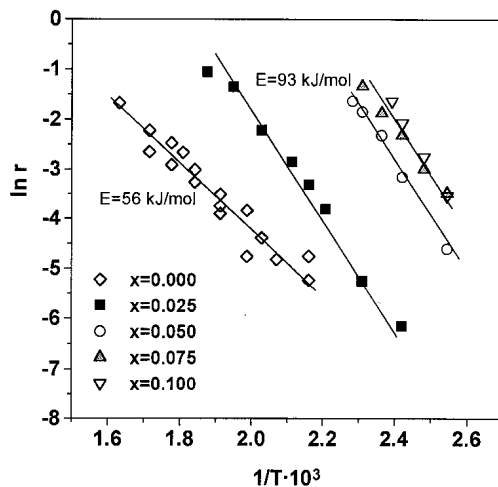


Fig. 6. Arrhenius plots of the global rate of CO oxidation on perovskite samples.

The specific surface area of all the synthesized samples was about $1 \text{ m}^2/\text{g}$. Therefore, the global rate of CO oxidation per gram or referred to the BET surface area of the catalysts is practically the same.

The global CO oxidation rates and specific rates calculated per surface ruthenium atom (taken from Table I), in Arrhenius form, are plotted in Fig. 6 and Fig. 7, respectively. As can be seen from Fig. 6, even a small substitution of Ru^{4+} for Cr^{3+} in the $\text{La}_{1-y}\text{Sr}_y\text{CrO}_3$ matrix results in an enhanced oxidation rate and in an increase of the apparent activation energy from 56 kJ to 93 kJ. The strontium chromate phase, stable to the temperature of 1250°C^{13} under oxidative conditions, present in all samples in approximately the same amount, is not essential for the activity. The global CO oxidation rate increases with further progressive substitution of Ru^{4+} for Cr^{3+} . However, the observed increase in the reaction rate does not follow the mole fraction of Ru (x) in the bulk of the samples. Almost the same global rate is obtained on the samples $\text{Ru}_{0.075}$ and $\text{Ru}_{0.100}$, with different degree of substitution of Ru in the bulk.

The XPS results (Table II) revealed not only higher Ru and Sr and lower Cr and La surface atomic concentrations in respect to those in the bulk, but also that samples $\text{Ru}_{0.075}$ and $\text{Ru}_{0.100}$ had very similar surface concentrations of ruthenium ions.

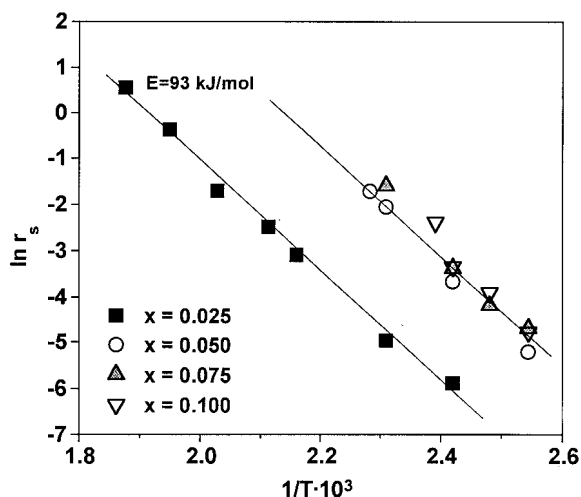


Fig. 7. Arrhenius plots of the specific rate of CO oxidation on perovskite samples.

These results indicated that surface Ru^{4+} ion have an essential influence on the overall activity. Moreover, samples with Ru mole fraction in the range $0.05 \leq x \leq 0.100$ exhibits nearly the same oxidation rate per Ru surface atom (Fig. 7). Since no other oxidation states of Ru were detected on the surface layers, the oxidation activity could be attributed to the Ru^{4+} ion.

The identical apparent activation energy $E = 93 \text{ kJ/mol}$ obtained on samples with a ruthenium content in the range $0.05 \leq x \leq 0.100$ and the very similar rate per ruthenium surface ion suggest that all the Ru sites are exposed and that mainly these

seats participate in the reaction. In accordance with the previous, it can be considered that no significant segregation of ruthenium on the surface occurs and that matrix effects arise from the fact that perovskite permits the high dispersion of Ru^{4+} .

It is interesting to realize the important difference in the specific activity of the sample with the lowest ruthenium content ($x = 0.025$). The significantly lower activity per ruthenium ion implies that not every exposed Ru^{4+} ions is active in CO oxidation. Since, the same apparent activation energy was obtained for this sample as for the samples with higher ruthenium contents, one of the possible explanations of this difference in activity could be found in the distance of the Ru ions in the perovskite phase. However, further work is necessary to clarify this point.

CONCLUSION REMARKS

The investigated catalysts, with the general formula $\text{La}_{1-y}\text{Sr}_y\text{Cr}_{1-x}\text{Ru}_x\text{O}_3$ ($0 \leq x \leq 0.100$), achieved a perovskite phase with about 20 % of SrCrO_4 . The amounts of metals, determined by XPS analysis of samples calcinated in air at 1000 °C, correspond to the stoichiometric values of the proposed chemical compositions. This proves that the incorporation of Ru into a perovskite matrix prevents the oxidation of ruthenium into volatile polyvalent oxides and their consequential escape from the samples up to 100 °C.

XPS data indicate a surface enrichment in Ru and Sr. It can, furthermore, be concluded that an increase in the global rate reflects the surface enrichment in Ru. The invariance of the apparent activation energy and the specific rate, computed per ruthenium surface atom in the samples, with a ruthenium content in the range $0.050 \leq x \leq 0.100$, suggest the Ru^{4+} ions are exposed and that they play a dominant role in the reaction.

Acknowledgment: Financial support from the Ministry of Science and Technology of the Republic of Serbia is gratefully acknowledged.

ИЗВОД

КАТАЛИТИЧКА СВОЈСТВА $\text{La}_{1-y}\text{Sr}_y\text{Cr}_{1-x}\text{Ru}_x\text{O}_3$ ПЕРОВСКИТА У ОКСИДАЦИЈИ УГЉЕНОМОКСИДА

А. ТЕРЛЕЦКИ-БАРИЧЕВИЋ, С. ПЕТРОВИЋ, Д. ЈОВАНОВИЋ, Љ. КАРАНОВИЋ* и Ц. МАРИНОВА**

ИХТМ Центар за катализу и хемијско инжењерство, Његошева 12, 11000 Београд, *Лабораторија за кристалографију, Рударско-геолошки факултет, Универзитета у Београду, Бушина 7, 11000 Београд,

**Институт за општу и неорганску хемију, БАН, 1113 Софија, Бугарска

Предмет овог рада је испитивање каталитичке активности мешаних оксида $\text{La}_{1-y}\text{Sr}_y\text{Cr}_{1-x}\text{Ru}_x\text{O}_3$ структуре перовскита са $y = 0,3$ и $0,025 \leq x \leq 0,100$ у оксидацији угљенмооксида. Висока сагласност унете и Х-флуоресцентном анализом нађене количине рутенијума у узорцима калцинисаним на 100 °C у ваздуху, указује на то да није дошло до значајне оксидације Ru до испарљивих поливалентних оксида и њиховог отпаравања из узорка. Анализа дифрактограма Х-зрака је показала да је у свим узорцима поред перовскитне

фазе присутан и мањи удео SrCrO_4 фазе. Концентрације Sr и Ru у површинским слојевима, израчунате из X-фотоелектронске спектроскопије, су веће у односу на њихову концентрацију у маси. Енергија везе Ru_{3p} је иста за све узорке и карактеристична је за Ru^{4+} . Кинетика оксидације угљенмоноксида испитивана је у диференцијалном рециркулатионом реактору. Резултати показују да делимична замена Cr^{3+} са Ru^{4+} у $\text{La}_{1-x}\text{Sr}_x\text{CrO}_3$ доводи до знатног пораста активности и енергије активације. Укупна брзина оксидација CO, обрачуната по јединици специфичне површине, је скоро пропорционална порасту атомске концентрације Ru^{4+} на површини узорка, односно $\text{Ru}_x \pm 0,05$ добивена је иста привидна енергија активације од $E = 93 \text{ kJ/mol}$ и иста специфична брзина оксидације по површинском јону Ru^{4+} , што указује на то да су јони Ru^{4+} изложени и да они превасходно учествују у реакцији.

(Примљено 6. јула 1999.)

REFERENCES

1. R. J. H. Voorhoeve, in *Advanced Materials in Catalysis*, J. J. Burton and R. C. Carter, Ed., Academic Press, New York, 1977, p. 129
2. B. Viswanathan, *Catal. Rev. - Sci. Eng.*, **34** (1992) 337
3. D. Jovanović, V. Dondur, A. Terlecki-Baričević, B. Grbić in *Catalysis and Automotive Pollution Control II*, (Studies in Surface Science and Catalysis Vol. 71), A. Crucq and A. Frennet, Eds., Elsevier, Amsterdam 1991, p. 371
4. R. Bradow, D. Jovanović, S. Petrović, Ž. Jovanović, A. Terlecki-Baričević, *Ind. Eng. Chem. Res.* **34** (1995) 1929
5. A. Terlecki-Baričević, *Materials Science Forum* **214** (1996) 115, Transtec Publications, Switzerland
6. A. Terlecki-Baričević, D. Jovanović, B. Grbić, S. Petrović, EPA Project "Perovskite Catalysts for Exhaust Gas Purification", Annual Report EPA-JF 885 (1991)
7. D. Jovanović, A. Terlecki-Baričević, B. Grbić, R. Bradow, U.S., Patent 5,318,937, June 7, 1994
8. R. G. Garvey, *Powder Diff.* **1** (1986) 114
9. P. Seah, M. T. Anthony, *Surf. Interf. Anal.* **6** (1984) 230
10. J. H. Scofield, *J. Electron Spectr. Related Phenom.* **8** (1976) 129
11. J. M. Berty, *Catal. Rev. - Sci. Eng.* **20** (1979) 75
12. A. Terlecki-Baričević, *Ph. D. Thesis*, Belgrade 1984
13. T. C. Gibb, M. Matsuo, *J. Solid Stat. Chem.* **86** (1990) 164
14. C. P. Khattak, D. E. Cox, *J. Appl. Cryst.* **10** (1977) 405
15. T. Seiyama, *Catal. Rev. - Sci. Eng.* **34** (1992) 281.